Received: 9 November 2021 | Revised: 12 January 2022 | Accepted: 24 January 2022

DOI: 10.1002/psp4.12769

ARTICLE

Covariate analysis of tusamitamab ravtansine, a DM4 anti-CEACAM5 antibody-drug conjugate, based on first-in-human study

Clemence Pouzin[1,2] | **Michel Tod**[2] | **Mustapha Chadjaa**[3] | **Nathalie Fagniez**[1] | **Laurent Nguyen**[1]

[1]Pharmacokinetics Dynamics and Metabolism Department, Sanofi R&D, Paris, France

[2]PKPD Modelling Unit, Oncology Department EMR3738, University of Claude Bernard Lyon 1, Lyon, France

[3]Clinical Research, Sanofi R&D, Paris, France

Correspondence
Clemence Pouzin, Pharmacokinetics Dynamics and Metabolism Department, Sanofi R&D, 1 Avenue Pierre Brossolette, 91380 Chilly-Mazarin, France.
Email: Clemence.Pouzin@sanofi.fr

Funding information
This study was funded by Sanofi R&D

Abstract

Tusamitamab ravtansine is an anti-CEACAM5 antibody-drug conjugate indicated in patients with solid tumors. Based on a previous developed semimechanistic model describing simultaneously pharmacokinetic (PK) of SAR408701, two of its active metabolites: DM4 and methyl-DM4 and naked antibody, with integration of drug-to-antibody data, the main objective of the present analysis was to evaluate covariate's impact in patients from phase I/II study ($n = 254$). Demographic and pathophysiologic baseline covariates were explored to explain interindividual variability on each entity PK parameter. Model parameters were estimated with good precision. Five covariates were included in the final PK model: body surface area (BSA), tumor burden, albumin, circulating target, and gender. Comparison of BSA-adjusted dosing and flat dosing supported the current BSA-based dosing regimen, to limit under and over exposure in patients with extreme BSA. Overall, this model characterized accurately the PKs of all entities and highlighted sources of PK variability. By integrating mechanistic considerations, this model aimed to improve understanding of the SAR408701 complex disposition while supporting key steps of clinical development.

Study Highlights

WHAT IS THE CURRENT KNOWLEDGE ON THE TOPIC?

Tusamitamab ravtansine (SAR408701) population pharmacokinetics (PKs) has been described by a semimechanistic PK model, characterizing simultaneously PK of SAR408701, two active metabolites: DM4 and methyl-DM4 (MeDM4), and naked antibody (NAB). This model included drug-to-antibody measurements and was successful in describing the PKs of all entities.

WHAT QUESTION DID THIS STUDY ADDRESS?

This study allowed to evaluate the impact of several demographic and pathophysiologic covariates on SAR408701, DM4, MeDM4, and NAB PKs simultaneously.

The sequential steps strategy was used that permitted avoiding potential interference between covariate effects on antibody-drug conjugate (ADC) and its derivatives.

WHAT DOES THIS STUDY ADD TO OUR KNOWLEDGE?

Semimechanistic complex models that help understanding ADC behavior are suitable for covariates research. By fixing some PK parameters from the structural model, the over running time can be circumvented.

HOW MIGHT THIS CHANGE DRUG DISCOVERY, DEVELOPMENT, AND/OR THERAPEUTICS?

This kind of semimechanistic analysis is applicable to other ADCs, which may differ from SAR408701 by payloads or linker properties and support drug development.

INTRODUCTION

Tusamitamab ravtansine (SAR408701) is a first-in-class humanized antibody-drug conjugate (ADC) that combines a monoclonal antibody (IgG1) and DM4, a potent maytansine derivative. SAR408701 is directed against carcinoembryonic antigen-related cell adhesion molecule 5 (CEACAM5), a cell-surface glycoprotein from the carcinoembryonic antigen family involved in cell adhesion, differentiation, proliferation, and survival.[1,2] This antigen is highly expressed in several epithelial tumors, such as colorectal cancer, lung, and gastric adenocarcinoma.

The payload (DM4) is covalently bound to the antibody via an N-succinimidyl 4-(2-pyridyldithio) butyrate (SPDB) linker, stable in plasma and cleavable inside cells. After SAR408701 binding to CEACAM5, DM4 is released inside cancer cells and rapidly methylated by an endogenous S-methyl transferase to form S-methyl-DM4 (MeDM4). DM4 and MeDM4 induce cytotoxicity by inhibition of cells proliferation at mitosis and suppression of microtubule dynamic instability.[3–6]

Preclinical data presented by Decary et al.[7] showed that SAR408701 appeared to be a promising candidate for clinical development. In the TED13751 phase I/II clinical study (https://clinicaltrials.gov/ct2/show/NCT02187848), SAR408701 presented encouraging antitumor activity in heavily pretreated patients with advanced nonsquamous non-small cell lung cancer (NSCLC) with high CEACAM5 expression (defined as ≥50% of the tumor cells per specimen with CEACAM5 positive staining at ≥2+ intensity). SAR408701, administered intravenously at 100 mg/m^2 every 2 weeks (q2w), led to an objective response rate of 20.3% and a favorable safety profile. Hematological toxicity was minimal compared to conventional chemotherapy and keratopathy appeared to be reversible and manageable with dose modification.[8] These results supported the launch of a phase III trial (https://clinicaltrials.gov/ct2/show/NCT04154956), evaluating the activity of SAR408701 monotherapy in comparison with docetaxel in nonsquamous NSCLC (CEACAM5 high expressors) after failure of standard first-line chemotherapy and anti-PD1/PD-L1.

Multiple analytes are considered when characterizing ADC pharmacokinetics (PKs). SAR408701 is administered intravenously as a conjugated antibody containing species with different payload densities: the number of cytotoxic molecules (i.e., DM4 molecules) per antibody is defined as the drug-to-antibody ratio (DAR). In the TED13751 study, SAR408701 (i.e., conjugated antibody with at least one payload: DAR ≥1), unconjugated DM4 and MeDM4 were measured in plasma, as well as naked antibody (NAB).

A semimechanistic population PK model has been developed by Pouzin et al. 2022,[9] describing SAR408701, DM4, MeDM4, NAB, and PK using data from 254 patients with CEACAM5-expressing solid tumors. Model details are presented in Online Resource 1.

The present analysis intended to identify potential covariates that may explain SAR408701, DM4, MeDM4, and NAB interindividual PK variability (IIV), evaluate the magnitude of covariates' impact on exposure, and compare dosing strategies based on this developed semimechanistic model.[9]

METHODS

Study design and patients

The population PK model was developed using clinical data from the TED13751 study. SAR408701 was administered as a single agent by intravenous infusion every 2 weeks (q2w; 1 cycle = 2 weeks) or every 3 weeks (q3w; 1 cycle = 3 weeks) in adult patients with advanced solid tumors. Doses ranged from 5 to 190 mg/m^2. Study cohorts and details can be found in Online Resource 2.

This study was approved by the Medical Ethics Committee and carried out in in accordance with the International Conference on Harmonization guidelines for Good Clinical Practice. All patients provided written informed consent.

Bioanalytical methods

The population PK model was built on plasma concentration of SAR408701 (determined by immunoassay quantifying conjugated antibody with at least one DM4 payload covalently bound), DM4 and MeDM4 (evaluated by liquid-chromatography assay coupled with tandem mass spectrometry), NAB (assessed by competitive immuno-enzymatic assay), and DAR (evaluated by liquid chromatography coupled with high resolution mass spectrometry).

The lower limit of quantification (LLOQ) was 0.5 μg/ml for SAR408701 and 0.2 ng/ml for DM4 and MeDM4. To avoid bioanalytical interference of SAR408701 on NAB quantification, samples were diluted to reach SAR408701 concentration below 15 μg/ml. Thus, the LLOQ for NAB varied from 1 to 9.60 μg/ml depending on SAR408701 concentration.

PK sampling was rich at cycle 1 and cycle 4, and predose samples were collected at intermediate cycles. Patients were treated over a maximum of 69 cycles, with a median of eight cycles per patient.

Population PK analysis

In the population PK model developed, PK data of SAR408701, NAB, DM4, MeDM4, average DAR, and proportions of individual DAR species over time were fitted simultaneously. The structural model is presented in Figure S1. Detailed development of the structural model can be found in Pouzin et al. 2021.[9]

Parameters were estimated using the parametric nonlinear mixed-effect modeling software Monolix (2020R1) with stochastic approximation expectation-maximization algorithm (SAEM) combined to the Markov Chain Monte Carlo procedure. Relative standard errors (RSEs) were calculated via estimation of the Fisher information matrix and log-likelihood calculation was estimated using importance sampling method. Pre and post data processing were performed with R software (version 3.6.1).

Model development

To avoid model overtime computing and overparameterization, some parameters from the final structural model were fixed during covariates research: deconjugation parameters ($k_{dec,i}$), DAR_i input fractions (F_{DARi}), and their associated IIV were set to estimated values from final structural model, and estimated only in the final model. As MeDM4, DM4, and NAB derive from SAR408701, covariates that impact SAR408701 PKs could also affect SAR408701 derivative PKs. To avoid such interference, covariates' impact was assessed in sequential steps.

In a first step, prior to covariate analysis, body surface area (BSA) impact, as a body size measure, was evaluated on all SAR408701 PK parameters (CL_{ADC}, V_c, Q, and V_p) to account for physiological changes within the population. BSA effect was first estimated, and then, if significant, fixed on relevant model parameters for the upcoming covariate analysis. Other covariates were then assessed first on SAR408701 model parameters alone (CL_{ADC}, V_c, Q, and V_p), with model adjusted on BSA effect. Impact of covariates (including BSA) was next estimated on NAB model parameter (CL_{NAB}), based on the model with fixed SAR408701 covariate effects. All covariates were finally evaluated on DM4 and MeDM4 model parameters (CL_{DM4}, CL_{MeDM4}, and FR_{MeDM4}), based on the model with fixed SAR408701 and NAB covariate effects. At the final step, all significant covariates and model parameters (including $k_{dec,i}$ and F_{DARi}) were estimated simultaneously.

Correlation between CL_{ADC} and V_c was investigated with partial variance-covariance matrix (all covariance elements being set to zero except for CL_{ADC}-V_c covariance). Final model selection was based on objective function (OF) value, Bayesian Information Criteria, precision of estimates (RSE), and visual inspection of overall goodness-of-fit (GOF) plots. The GOF plots regrouped plots of observed concentrations versus model population and individual predicted concentrations, as well as population and individual weighted residuals (PWRES and iWRES) versus time and versus model predicted concentrations. To internally qualify the final model, inspection of prediction-corrected visual predictive check (pc-VPC)[10] plots and normal prediction distribution error (NPDE)[11] plots were also used.

Covariate selection

Clinically relevant demographic and pathophysiologic covariates (presented in Online Resource 3) were investigated on each entity PK parameters using a stepwise forward addition followed by backward deletion. A change in OF value with statistical criteria of $p < 0.05$ (log-likelihood ratio test) was used for the forward addition step. The full model was determined with significant covariates at Wald test with statistical criteria of $p < 0.05$. For the backward deletion step, statistical criteria of $p < 0.001$ was needed to retain covariates in the final model.

The parameter-covariate relationship was modeled for continuous covariates (e.g., BSA) as follows:

$$P_i = P_{TV} \times \frac{BSA_i}{BSA_{median}}^{\beta_{BSA}} \times e^{\eta_{P,i}}$$

where P_i is the individual value of a parameter with individual random effect $e^{\eta_{P,i}}$, for an individual i with a body surface area BSA_i, P_{TV} is the parameter typical value for a typical individual with median body surface area BSA_{median}, and β_{BSA} is the estimated exponent quantifying BSA impact on P_{TV}.

Categorical covariates (e.g., gender) were tested as follow:

$$P_i = P_{TV} \times \beta_{GENDER}^{GENDER} \times e^{\eta_{P,i}}$$

where P_i is the individual value of a parameter with individual random effect $e^{\eta_{P,i}}$, for an individual i with a body surface area BSA_i, P_{TV} is the parameter typical value for a typical male individual (GENDER = 0 for men and GENDER = 1 for women). β_{GENDER} is the estimated coefficient quantifying female impact on P_{TV}.

Covariates' impact and model-based simulations

Covariate effect was evaluated on PK and exposure parameters.

Typical PK simulations were performed to assess covariates impact on exposure for each active entity (SAR408701, DM4, and MeDM4). The final model was used to simulate 100 mg/m² q2w dosing for a typical patient (i.e., with typical parameter values). Area under the concentration versus time curve between two administrations (AUC_{TAU}) and maximum concentration (C_{max}) were derived at steady-state.

For continuous covariates, patients with 5th percentile, median (i.e., reference patient) and 95th percentile values of covariate distribution were simulated, and for categorical covariates, patients in each covariate subclass were simulated (all other covariates being set to median values). Results were expressed as parameter percentage change from reference patient estimate. Sensitivity plots were performed to compare typical covariates effect at steady-state with individual exposures of the entire population.

Flat dose simulations

Estimated individual parameters from final population model were used to simulate two dosing scenarios, to compare variability between BSA adjusted dosing regimen and flat dosing.

Typical BSA based dosing (100 mg/m² q2w, with BSA capped at 2.20 m² for greater BSA) and flat dosing (180 mg q2w, calculated for a typical 1.80 m² patient) were simulated. SAR408701 AUC_{TAU} and C_{max} were calculated at steady-state for each dosing scenario (no effect of BSA on PK parameters of DM4 and MeDM4 was observed, thus impact was not evaluated on these entities). Deviation from median value of BSA based dosing of each parameter was quantified. Results were presented as boxplots of parameter distribution by BSA quartiles subgroups.

RESULTS

Patients characteristics and observed data

Final dataset for population PK analysis included 254 patients from the TED13751 study (study details presented in Online Resource 2). A total of 3726 SAR408701 plasma concentrations, 3722 DM4 plasma concentrations, 3728 MeDM4 plasma concentrations, and 3717 NAB plasma concentrations were included in the analysis. Data below the limit of quantification (BLOQ), represented 1%, 36%, 13%, and 31% of total SAR408701, DM4, MeDM4, and NAB concentrations respectively. BLOQ data were handled as left-censored data by Monolix and imputed using likelihood-based approach (equivalent to M3 method in NONMEM): the SAEM algorithm computed the maximum likelihood estimate of the population parameters combining censored and noncensored data information.

Baseline patient characteristics are presented in Table S3 and Table S4 (Online Resource 3) and regrouped demographic covariates (age, gender, ethnic, race, and body size measures), creatinine clearance, laboratory values of albumin (ALB), bilirubin (BILI), total protein, ASAT, ALAT, and tumor-related covariates. Among tumor-related covariates: CEACAM5 tumoral expression, assessed at the membrane by immunohistochemistry as the percentage of tumoral cells expressing the target with intensity greater than 2+ (CEACAM5); H-SCORE, defined for tumor cells as the sum of three times the percentage of 3+ cells, two times the percentage of 2+ cells, and one times the percentage of 1+ cells; tumor burden (TMBD) according to RECIST 1.1[12] (i.e., sum of the longest dimension of target lesions); circulating CEA (SHED); Eastern Cooperative Oncology Group status (ECOG), and tumor type were reported. ADC being internalized after target binding and these specific covariates may affect SAR408701 PKs. TMBD ranged from 11.0 to 339 mm, with a median of 84.0 mm in the studied population. SHED distribution was wide

and revealed high variability with values ranging from 500 to 41,227,000 pg/ml. Percentage of CEACAM5 tumoral expression ranged from 0% to 100% with a median of 70%. No correlation was found between theses tumor-related covariates.

Final population PK model

Covariates were tested on each entity clearance (CL_{ADC}, CL_{NAB}, CL_{DM4}, and CL_{MeDM4}), on SAR408701 and NAB distribution volumes (V_c and V_p), and on MeDM4 input fraction (FR_{MeDM4}).

As body weight (BW), body mass index, and BSA were highly correlated (body size measures), BSA was considered as the reference body size covariate. The final model included BSA impact (positive correlation) on SAR408701 proteolytic clearance (CL_{ADC}) and distribution volumes (V_c and V_p). Thus, no remaining correlation with other body size associated covariates was found in the final model. BSA was not found to affect other entities PK parameters.

After forward addition and backward deletion, final significant covariates (with either positive or negative correlation) impacting model parameters and explaining part of IIV (ω) from final structural model were:

- BSA (+), ALB (−), and TMBD (+) on CL_{ADC} (IIV decrease from 46.9% to 33.0% on CL_{ADC})
- BSA (+), ALB (−), and TMBD (+) on V_c (IIV decrease from 24.5% to 16.0% on V_C)
- BSA (+) and SHED (+) on V_p (IIV decrease from 60.5% to 50.9% on V_p)
- SEX (−) on CL_{DM4} (IIV decrease from 36.5% to 34.6% on CL_{DM4})
- ALB (+) and TMBD (−) on CL_{MeDM4} (IIV decrease from 65.4% to 55.6% on CL_{MeDM4})
- ALB (−) and SHED (+) on FR_{MeDM4} (IIV decrease from 72.3% to 59.7% on FR_{MeDM4})

Parameter-covariates relations included in the final model and final model parameters are presented in Online Resource 4. After covariates' inclusion, SAR408701 proteolytic clearance was estimated at 0.410 L/day. Distribution volumes were estimated at 3.31 L for V_c and 2.66 L for V_p, respectively. DM4 and MeDM4 apparent clearances were estimated at 253 L/day and 0.248 L/day, respectively. IIV on MeDM4 PK parameters was much larger than that of other entities' PK parameters, with IIV reaching 59.7% for FR_{MeDM4} and 55.6% for CL_{MeDM4}, whereas IIV ranged from 33.0% for CL_{ADC} to 34.6% for CL_{DM4}.

Model qualification

GOF plots and NPDE evaluating model performance are presented in Online Resource 5. Plots of observations versus population predictions and observations versus individual predictions indicated that the model adequately described the observations of each entity over the dose range. Population or individual weighted residuals (PWRES and iWRES), and NPDE versus time or versus model prediction plots were well distributed with a random distribution around zero. Parameter correlations between model parameters (presented in Online Resource 6 – 1) confirmed that no correlation remained in final model. Pc-VPC plots for SAR408701 (Figure 1) and for other entities (Online Resource 7) showed that simulations were able to describe accurately observed concentrations in the current dose range.

Covariates' impact

Effect of extreme values of significant covariates was assessed on relevant PK parameters, and relative changes of each parameter are presented in Table S6 (Online Resource 8).

Covariates impact on exposure was assessed for all active entities (i.e., SAR408701, DM4, and MeDM4) after 100 mg/m² q2w dosing. Exposure parameters (i.e., AUC_{TAU} and C_{max}) at steady-state were derived after typical simulations for each covariate extreme values (i.e., 5th and 95th percentiles). Results were expressed as percentage change from reference value (i.e., median value for BSA, ALB, TMBD, and SHED or men for SEX).

Sensitivity plots suggested that TMBD and ALB were the most impactful covariates on SAR408701 exposure (Figure 2a. for AUC_{TAU} and Figure S5a. for C_{max} in Online Resource 8). Typical simulations are presented Figure 3 for TMBD extreme values. Patients with low TMBD showed higher SAR408701 exposure (+39.5% change of AUC_{TAU}), whereas patients with high TMBD displayed lower SAR408701 exposure (−17.7% change of AUC_{TAU}). ALB impact on SAR408701 ranged from −29.5% for patients with low ALB to +19.7% for patients with high ALB. No impact of SHED, BSA, and SEX on SAR408701 exposure was found (<3%).

On DM4 exposure, overall, covariate influence was quantified with less than 30% change for all significant covariates (Figure 2b and Figure S5b). BSA and SEX were the most influential covariates, with −18.0%/+21.1% change of AUC_{TAU} for patients with low/high BSA, and +27.2% change of AUC_{TAU} for women compared with men.

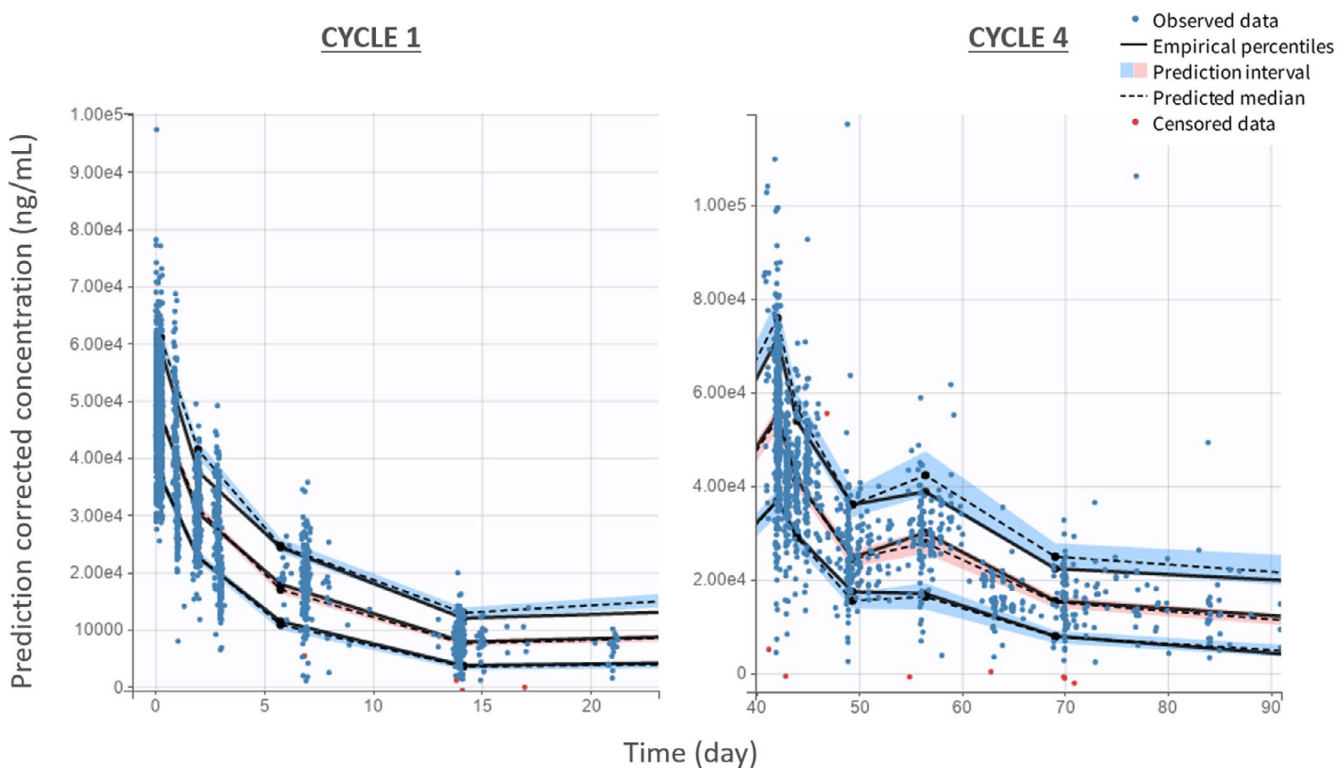

FIGURE 1 Tusamitamab ravtansine (SAR408701) prediction corrected visual predictive check at cycle 1 and cycle 4. The points represent the observed concentrations (in red the below the limit of quantification values, handled as censored data), the solid lines represent the median, 10th and 90th percentiles of the observed data, and the blue and red areas represent the prediction intervals for each percentile (at a level of 90%)

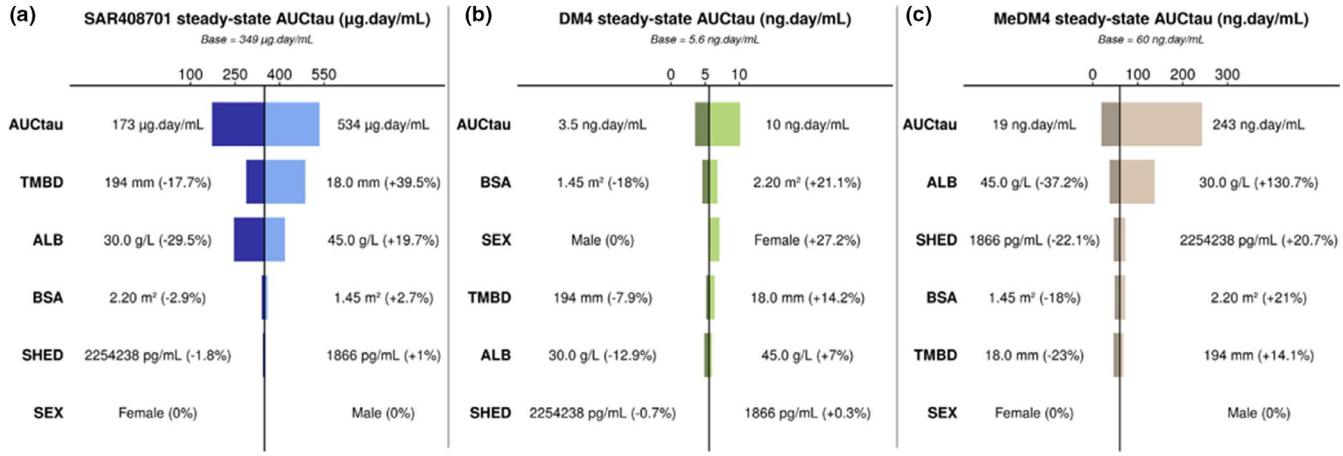

FIGURE 2 Sensitivity plots comparing covariates impact on AUC_{TAU} at steady-state of SAR408701 (a), DM4 (b), and MeDM4 (c). "Base" represents typical exposure parameter value (i.e., typical male patient with median covariates values). AUC_{TAU} ranges are represented for 5th to 95th percentiles of individual simulations in the entire population. Covariate ranges are represented for typical simulation of 5th and 95th percentiles of each covariate distribution, with percentiles values (% change from reference). ALB, albumin; AUC_{TAU}, area under the concentration versus time curve between two administrations; BSA, body surface area; MeDM4, methyl-DM4; SAR408701, tusamitamab ravtansine; TMBD, tumor burden

MeDM4 sensitivity plots (Figure 2c and Figure S5c) evidenced that ALB was the most impactful covariate on MeDM4 profiles. Typical simulations are presented in Figure 4 for ALB extreme values. Patients with low ALB showed higher MeDM4 exposure, with more than +130.7% change of AUC_{TAU}, whereas patients with high ALB showed lower exposure (−37.2%). SHED, BSA, and TMBD had limited influence on MeDM4, with less than

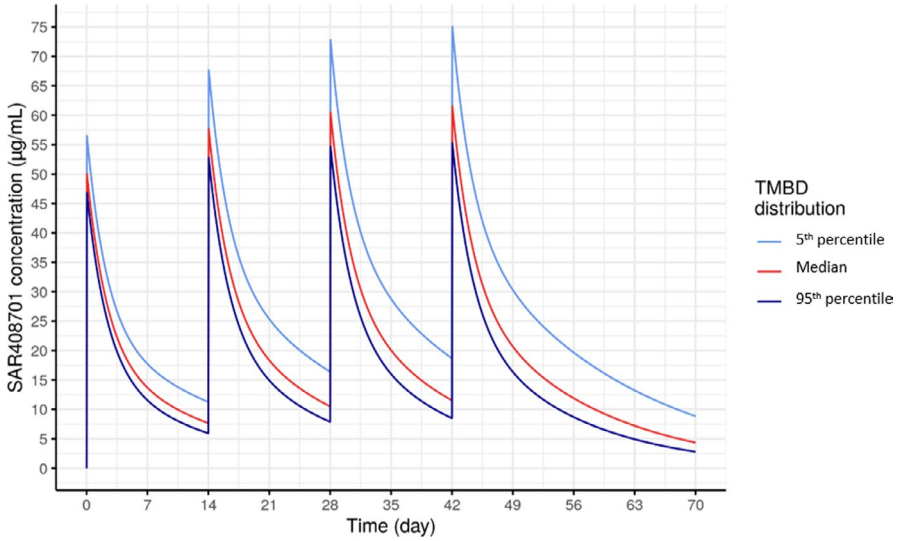

FIGURE 3 TMBD impact on SAR408701 typical PK profile. Simulations were performed for a typical patient (i.e., typical male patient with median covariates values). PK, pharmacokinetic; SAR408701, tusamitamab ravtansine; TMBD, tumor burden

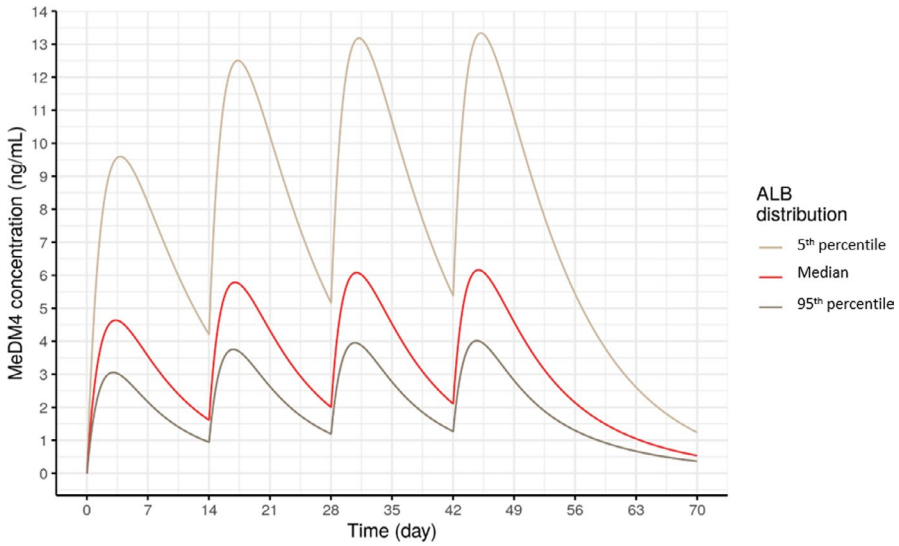

FIGURE 4 ALB impact on MeDM4 typical PK profile. Simulations were performed for a typical patient (i.e., typical male patient with median covariates values). ALB, albumin; MeDM4, methyl-DM4; PK, pharmacokinetic

23% change of AUC_{TAU} parameter for extreme covariate values: patients with low TMBD and SHED displayed lower MeDM4 exposure whereas patients with high TMBD and SHED showed higher exposure. BSA impact ranged from −18% change (for patients with low BSA) to +21% change of AUC_{TAU} (for patients with high BSA).

Flat dose simulation

Boxplots of SAR408701 AUC_{TAU} and C_{max} calculated after 100 mg/m² q2w (with BSA capped at 2.20 m²) or 180 mg q2w flat dosing are presented in Figure 5. Values are expressed as percentage change from median value of BSA based dosing and represented by quartiles of BSA distribution in the entire population.

With BSA-based dosing, no change in exposure at steady-state across quartiles subgroups was evidenced. Whereas with flat dosing, patients with low BSA (i.e., patients with BSA < BSA_{Q1}) were higher exposed and patients with high BSA (i.e., patients with BSA > BSA_{Q3}) tended to be lower exposed.

DISCUSSION

The present population PK analysis pictures the first covariates assessment of SAR408701, based on a semi-mechanistic model characterizing simultaneously PKs of SAR408701 (i.e., conjugated ADC with at least one payload), DM4, MeDM4 (active metabolites), and NAB. This model considered DAR (structural model presented by Pouzin et al.[9]) and was successful in describing PKs of all entities in the studied population (254 patients with solid tumor from TED13751 study). Covariates were investigated concomitantly on each entity.

Out of all approved ADCs, only a few published models included DAR measurements. In fact, immunoassays

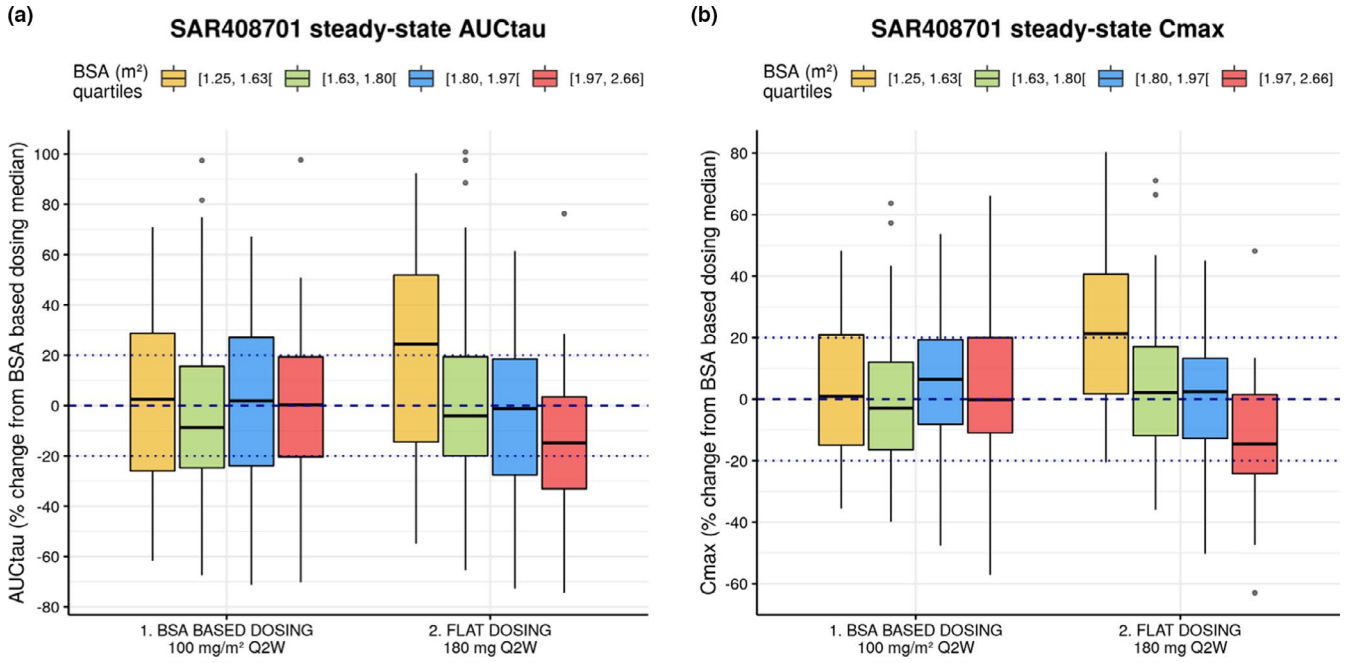

FIGURE 5 BSA based dosing and flat dosing impact on SAR408701 exposure at steady-state. Boxplots (by BSA quartiles) of SAR408701 individual values of AUC_{TAU} and C_{max}, calculated after 100 mg/m² q2w (with BSA capped at 2.20 m²) or 180 mg q2w flat dosing. AUC_{TAU}, area under the concentration versus time curve between two administrations; BSA, body surface area; C_{max}, maximum concentration; SAR408701, tusamitamab ravtansine

usually capture total or conjugated antibody but fail to differentiate ADC components with different loads. Improvements in the bioanalytical field[13] allowed distinction of ADC moieties with characterization of the number of payloads linked to each ADC. Consideration of DAR in population PK models allows to enhance the understanding of ADCs' complex behaviors and strengthen confidence in mechanistic hypothesis governing ADCs' disposition.[14,15] But such models are complex, require many parameters to estimate (DAR input fractions and deconjugation rate constants), and exhibit important run time, which may limit their use.

Our model, in addition to DAR consideration, fitted simultaneously metabolites' PK data. Payloads' plasma behavior is of interest as they may be related to safety or efficacy concerns. Cytotoxic PKs is usually described when circulating concentrations are quantifiable, which is not always the case: for inotuzumab ozogamicin and trastuzumab emtansine ADCs, levels of unconjugated calicheamicin and DM1 being generally BLOQ, PK was not reported for these payloads in published population PK models.[16,17] For other approved ADCs, payload PKs are reported either in separate models, or in integrated models where ADC and cytotoxic concentrations are described together.[18] The present analysis is the first semimechanistic model (including DAR measurement) which evaluate covariates impact on SAR408701 ADC and its derivatives simultaneously.

Five covariates were found to significantly impact PK parameters and thus decrease IIV on related parameters: BSA, ALB, SHED, TMBD, and SEX. Other covariates studied (including age, ethnic, race, creatinine clearance, bilirubin, total protein, ASAT, ALAT, percentage of CEACAM5 tumoral expression, HSCORE, ECOG, and tumor type) were not significant. To avoid interference between covariates' effect on SAR408701 and its derivatives, covariates' research was performed with sequential steps: first identified on SAR408701, then on NAB, DM4, and MeDM4. At the final step, significant covariates and model parameters were estimated simultaneously for all entities. Values in this final step of estimated parameters and covariate coefficients were close to those found in the sequential steps process, which strengthened confidence in the final model estimates.

Correlations between parameters were explored with final developed model (Online Resource 6 – 1). Only CL_{ADC} and V_c parameters resulted to be correlated (correlation estimated at 0.565). No correlation was found among ADC and DM4, MeDM4, or NAB parameters. Each entity clearance was independent to each other (Person's correlation coefficient estimates lower than 0.32).

BSA impacted SAR408701 proteolytic clearance and distribution volumes with allometric coefficients of 1.09 (on CL_{ADC}), 1.03 (on V_c), and 1.65 (on V_p). The change in PK parameters (CL_{ADC}, V_c, and V_p) for extreme BSA values (5th and 95th percentiles; Online Resource 8) ranged

from −30.0% to +39.3%. However, BSA-based dosing limited its effect on SAR408701 exposure (<3% change of SAR408701 AUC_{TAU} at steady-state). BSA impact on DM4 and MeDM4 was higher, with around 20% change of metabolites AUC_{TAU} parameters, but these variations were limited and remained within the global interpatient variability observed in DM4 and MeDM4 profiles.

Simulations of corresponding flat dosing regimen (i.e., 180 mg q2w) showed that extreme BSA patients would result in either higher exposure (for patients with low BSA) or lower exposure (for patients with high BSA). Patients with low BSA could incur a safety concern, as exposure would increase by +50% (change of AUC_{TAU}). Thus, the current dosing regimen based on BSA adjustment is appropriate to avoid exposure disparity in patients with extreme BSA and limit potential clinical impact in regard of safety or efficacy.

BSA or BW are commonly identified as key covariates affecting ADC PK parameters. Exponential impact of such weight-related covariates is included in all PK models of published ADCs.[18] Allometric exponents can be fixed to their theoretical values[19]**:** 1 for volumes and 0.75 for clearances (e.g., gemtuzumab ozogamicin[20]), but they usually are estimated (e.g., inotuzumab ozogamicin,[21] trastuzumab emtansine,[22] and polatuzumab vedotin[23]). On Li et al.[24] integrated two-analytes PK model, BW effect was fixed on metabolite PK parameters but estimated on ADC parameters. Overall, weight-related covariates reduce significantly IIV on PK parameters. Thus, BW or BSA-based dosing is always considered as the reference for ADC dosing.

A significant model covariate was ALB. Patients with low ALB had higher SAR408701 proteolytic clearance values (+49.4% change of CL_{ADC}) and thus lower SAR408701 exposure (−29.5% change of AUC_{TAU} at steady-state) compared to reference patients. This finding was expected because ALB reflects global protein catabolism: chronic systemic inflammatory condition observed in patients with cancer leads to cachexia and elevated protein turnover, which induces hypoalbuminemia. Endogenous catabolic rate of ALB being highly correlated with IgG turnover, increased protein turnover results in a high catabolic degradation of IgG and an enhance of systemic ADC clearance.[25] ALB is thus a potential prognostic factor: higher serum levels have been associated with better survival.[26] Inverse correlation between ALB levels and biologics clearance is widely described for monoclonal antibodies[25,27] and multiple approved ADCs (e.g., trastuzumab emtansine,[28,29] gemtuzumab ozogamicin,[20] brentuximab vedotin,[30] and polatuzumab vedotin[23]).

ALB was a covariate impacting as well MeDM4 formation and elimination, with +84.4% change of FR_{MeDM4} and −29.3% change of CL_{MeDM4} for patients with low ALB, conducting to higher MeDM4 exposure (+130.7% change of AUC_{TAU}). Full explanation of such effect is not completely elucidated; however, some interpretations can be made. Increase of MeDM4 exposure may be related to enhanced SAR408701 degradation and payload release (+49.4% change of CL_{ADC}). Moreover, MeDM4 is known to be metabolized in the liver by cytochromes leading to formation of sulfoxide and sulfone derivatives that are excreted into the bile.[31,32] Hypoalbuminemia could reflect liver impairment, which would alter cytochrome activity and thus MeDM4 elimination.

Sensitivity analysis allowed to quantify and compare covariates' impact on exposure in regard of individual exposures in the studied population. MeDM4 profiles exhibited strong IIV, with AUC_{TAU} values ranging from 19 to 243 ng.day/ml and C_{max} values ranging from 2.3 to 23 ng/ml. Observed MeDM4 overexposure (+130.7%) in patients with low ALB remained within the global IIV observed in treated patients. Moreover, preliminary analysis (data not published) suggested that the main dose limiting toxicity event (i.e., corneal event) was related to SAR408701 exposure, and not to metabolites. These results suggested that hypoalbuminemia and its impact on MeDM4 exposure would not result in major safety concern. However, deeper analyses are to be conducted to identify and confirm safety drivers within the SAR408701 derivatives.

Another covariate affecting PK was TMBD. Baseline tumor burden affected SAR408701 proteolytic clearance and MeDM4 apparent clearance over a range of −33.9%/+25.2% change of CL_{ADC} and +48.1%/−19.2% change of CL_{MeDM4} (TMBD 5th/95th percentile). Correlations between model parameters were explored (Online Resource 6 – 2) and revealed that CL_{ADC} and CL_{MeDM4} were not correlated with each other. Moreover, no correlation between k_{dec} parameter and TMBD was found. Thus, the tumor burden affected independently ADC and MeDM4 elimination processes. Patients with high TMBD were lower exposed to SAR408701 (−17.7% change of AUC_{TAU} at steady-state) and higher exposed to MeDM4 (+14.2%). Even if the full mechanism is still unclear, high tumor burden may lead to a higher target-mediated drug clearance, by increased ADCs internalization and processing (decrease of SAR408701 AUC_{TAU}), and thus enhanced metabolites formation (increase of MeDM4 AUC_{TAU}).

This is the first analysis that integrates mechanistic consideration to fit population PKs of SAR408701 and its derivatives in patients with cancer to identify covariates effect. This model aimed to improve understanding of SAR408701 complex disposition while determining sources of PK variability to support drug clinical development. This kind of semimechanistic analysis is applicable to other ADCs, which may differ from SAR408701

by payloads or linker properties and support drug development.

ACKNOWLEDGEMENTS

The authors thank Tracy Harrison of in Science Communications, Springer Healthcare, for assistance with manuscript styling prior to submission. This assistance was funded by Sanofi Genzyme.

CONFLICT OF INTEREST

The authors declared no competing interests for this work.

AUTHOR CONTRIBUTIONS

C.P. wrote the manuscript. N.F., L.N., and M.C. designed the research. C.P. performed the research. C.P., L.N., and M.T. analyzed the data.

REFERENCES

1. Hammarström S. The carcinoembryonic antigen (CEA) family: structures, suggested functions and expression in normal and malignant tissues. *Semin Cancer Biol*. 1999;9:67-81.
2. Taheri M, Saragovi U, Fuks A, Makkerh J, Mort J, Stanners CP. Self recognition in the Ig superfamily. Identification of precise subdomains in carcinoembryonic antigen required for intercellular adhesion. *J Biol Chem*. 2000;275:26935-26943.
3. Oroudjev E, Lopus M, Wilson L, et al. Maytansinoid-antibody conjugates induce mitotic arrest by suppressing microtubule dynamic instability. *Mol Cancer Ther*. 2010;9:2700-2713.
4. Lopus M, Oroudjev E, Wilson L, et al. Maytansine and cellular metabolites of antibody-maytansinoid conjugates strongly suppress microtubule dynamics by binding to microtubules. *Mol Cancer Ther*. 2010;9:2689-2699.
5. Erickson HK, Park PU, Widdison WC, et al. Antibody-maytansinoid conjugates are activated in targeted cancer cells by lysosomal degradation and linker-dependent intracellular processing. *Cancer Res*. 2006;66:4426-4433.
6. Erickson HK, Widdison WC, Mayo MF, et al. Tumor delivery and in vivo processing of disulfide-linked and thioether-linked antibody-maytansinoid conjugates. *Bioconjug Chem*. 2010;21:84-92.
7. Decary S, Berne P-F, Nicolazzi C, et al. Preclinical activity of SAR408701: a novel Anti-CEACAM5-maytansinoid antibody-drug conjugate for the treatment of CEACAM5-positive epithelial tumors. *Clin Cancer Res*. 2020;26:6589-6599.
8. Gazzah A, Ricordel C, Cousin S, et al. Efficacy and safety of the antibody-drug conjugate (ADC) SAR408701 in patients (pts) with non-squamous non-small cell lung cancer (NSQ NSCLC) expressing carcinoembryonic antigen-related cell adhesion molecule 5 (CEACAM5). *J Clin Oncol*. 2020;38:9505.
9. Pouzin C, Gibiansky L, Fagniez N, et al. Integrated multiple analytes and semi-mechanistic population pharmacokinetic model of tusamitamab ravtansine, a DM4 anti-CEACAM5 antibody-drug conjugate. *J Pharmacokinet Pharmacodyn*. 2022. https://doi.org/10.1007/s10928-021-09799-0
10. Bergstrand M, Hooker AC, Wallin JE, Karlsson MO. Prediction-corrected visual predictive checks for diagnosing nonlinear mixed-effects models. *AAPS J*. 2011;13:143-151.
11. Comets E, Brendel K, Mentré F. Computing normalised prediction distribution errors to evaluate nonlinear mixed-effect models: the npde add-on package for R. *Comput Methods Programs Biomed*. 2008;90:154-166.
12. Eisenhauer EA, Therasse P, Bogaerts J, et al. New response evaluation criteria in solid tumours: revised RECIST guideline (version 1.1). *Eur J Cancer*. 2009;45:228-247.
13. Zhu X, Huo S, Xue C, An B, Qu J. Current LC-MS-based strategies for characterization and quantification of antibody-drug conjugates. *J Pharm Anal*. 2020;10:209-220.
14. Gibiansky L, Gibiansky E. Target-mediated drug disposition model and its approximations for antibody-drug conjugates. *J Pharmacokinet Pharmacodyn*. 2014;41:35-47.
15. Chudasama VL, Schaedeli Stark F, Harrold JM, et al. Semi-mechanistic population pharmacokinetic model of multivalent trastuzumab emtansine in patients with metastatic breast cancer. *Clin Pharmacol Ther*. 2012;92:520-527.
16. Australian Public Assessment Report for Inotuzumab ozogamicin. 2019:115.
17. Lambert JM, Chari RVJ. Ado-trastuzumab Emtansine (T-DM1): an antibody–drug conjugate (ADC) for HER2-positive breast cancer. *J Med Chem*. 2014;57:6949-6964.
18. Liu SN, Li C. Clinical pharmacology strategies in supporting drug development and approval of antibody–drug conjugates in oncology. *Cancer Chemother Pharmacol*. 2021;87:743-765.
19. West G, Brown J, Enquist B. The fourth dimension of life: fractal geometry and allometric scaling of organisms. *Science*. 1999;284:1677-1679.
20. Hibma J, Knight B. Population pharmacokinetic modeling of gemtuzumab ozogamicin in adult patients with acute myeloid leukemia. *Clin Pharmacokinet*. 2019;58:335-347.
21. Garrett M, Ruiz-Garcia A, Parivar K, Hee B, Boni J. Population pharmacokinetics of inotuzumab ozogamicin in relapsed/refractory acute lymphoblastic leukemia and non-Hodgkin lymphoma. *J Pharmacokinet Pharmacodyn*. 2019;46:211-222.
22. Lu D, Girish S, Gao Y, et al. Population pharmacokinetics of trastuzumab emtansine (T-DM1), a HER2-targeted antibody–drug conjugate, in patients with HER2-positive metastatic breast cancer: clinical implications of the effect of covariates. *Cancer Chemother Pharmacol*. 2014;74:399-410.
23. Lu D, Lu T, Gibiansky L, et al. Integrated two-analyte population pharmacokinetic model of polatuzumab vedotin in patients with non-Hodgkin lymphoma. *CPT Pharmacometrics Syst Pharmacol*. 2020;9:48-59.
24. Li H, Han TH, Hunder NN, Jang G, Zhao B. Population pharmacokinetics of brentuximab vedotin in patients with CD30-expressing hematologic malignancies. *J Clin Pharmacol*. 2017;57:1148-1158.
25. Ryman JT, Meibohm B. Pharmacokinetics of monoclonal antibodies. *CPT Pharmacometrics Syst Pharmacol*. 2017;6:576-588.
26. Gupta D, Lis CG. Pretreatment serum albumin as a predictor of cancer survival: a systematic review of the epidemiological literature. *Nutr J*. 2010;9:69.
27. Mould DR, Meibohm B. Drug development of therapeutic monoclonal antibodies. *BioDrugs*. 2016;30:275-293.
28. Cosson VF, Ng VW, Lehle M, Lum BL. Population pharmacokinetics and exposure–response analyses of trastuzumab in patients with advanced gastric or gastroesophageal junction cancer. *Cancer Chemother Pharmacol*. 2014;11:737-747.
29. Gupta M, LoRusso PM, Wang B, et al. Clinical implications of pathophysiological and demographic covariates on the population

pharmacokinetics of Trastuzumab Emtansine, a HER2-targeted antibody-drug conjugate, in patients with HER2-positive metastatic breast cancer. *J Clin Pharmacol*. 2012;52:691-703.
30. Suri A, Mould DR, Liu Y, Jang G, Venkatakrishnan K. Population PK and exposure-response relationships for the antibody-drug conjugate Brentuximab Vedotin in CTCL patients in the Phase III ALCANZA Study. *Clin Pharmacol Ther*. 2018;104:989-999.
31. Sun X, Widdison W, Mayo M, et al. Design of antibody-maytansinoid conjugates allows for efficient detoxification via liver metabolism. *Bioconjug Chem*. 2011;22:728-735.
32. Davis JA, Rock DA, Wienkers LC, Pearson JT. In vitro characterization of the drug-drug interaction potential of catabolites of antibody-maytansinoid conjugates. *Drug Metab Dispos*. 2012;40:1927-1934.

SUPPORTING INFORMATION

Additional supporting information may be found in the online version of the article at the publisher's website.

How to cite this article: Pouzin C, Tod M, Chadjaa M, Fagniez N, Nguyen L. Covariate analysis of tusamitamab ravtansine, a DM4 anti-CEACAM5 antibody-drug conjugate, based on first-in-human study. *CPT Pharmacometrics Syst Pharmacol*. 2022;11:384-394. doi:10.1002/psp4.12769